Paper 32

Porphyry Indicator Minerals (PIMS) and Porphyry Vectoring and Fertility Tools (PVFTS) – Indicators of Mineralization Styles and Recorders of Hypogene Geochemical Dispersion Halos

Cooke, D.R. [1,2], Agnew, P. [3], Hollings, P. [4], Baker, M. [1,2], Chang, Z. [5], Wilkinson, J.J. [6,7], White, N.C. [2,8], Zhang, L. [1,2], Thompson, J. [1,2], Gemmell, J.B. [1,2], Fox, N. [2], Chen, H. [9], Wilkinson, C.C. [6]

1. Transforming the Mining Value Chain, an ARC Industrial Transformation Research Hub, University of Tasmania, Private Bag 79. Hobart, Tasmania, 7001, Australia
2. CODES, the Australian Research Council's Centre for Excellence in Ore Deposits, University of Tasmania, Private Bag 79. Hobart, Tasmania, 7001, Australia
3. Rio Tinto Exploration, Research Avenue, Bundoora, Victoria, 3083, Australia
4. Geology Department, Lakehead University, 955 Oliver Road, Thunder Bay, Ontario, Canada P7B 5E1
5. EGRU (Economic Geology Research Centre) and Academic Group of Geosciences, College of Science and Engineering, James Cook University, Townsville, Queensland 4811, Australia.
6. LODE, Department of Earth Sciences, Natural History Museum, London SW7 5BD, UK;
7. Department of Earth Science & Engineering, Imperial College London, Exhibition Road, London SW7 2AZ
8. Ore Deposit and Exploration Centre (ODEC), School of Resources and Environmental Engineering, Hefei University of Technology, Hefei 230009, Anhui, China
9. Guangzhou Institute of Geochemistry, Chinese Academy of Sciences, 511 Kehua Street, Tianhe, PO Box 1131, Guangzhou, China, 510640

ABSTRACT

In the past decade, significant research efforts have been devoted to mineral chemistry studies to assist porphyry exploration. These activities can be divided into two major fields of research: (1) porphyry indicator minerals (PIMS), which aims to identify the presence of, or potential for, porphyry-style mineralization based on the chemistry of magmatic minerals such as plagioclase, zircon and apatite, or resistate hydrothermal minerals such as magnetite; and (2) porphyry vectoring and fertility tools (PVFTS), which use the chemical compositions of hydrothermal minerals such as epidote, chlorite and alunite to predict the likely direction and distance to mineralized centres, and the potential metal endowment of a mineral district. This new generation of exploration tools has been enabled by advances in laser ablation-inductively coupled plasma mass spectrometry, short wave length infrared data acquisition and data processing, and the increased availability of microanalytical techniques such as cathodoluminescence. PVFTS and PIMS show considerable promise for porphyry exploration, and are starting to be applied to the diversity of environments that host porphyry and epithermal deposits around the circum-Pacific region. Industry has consistently supported development of these tools, in the case of PVFTS encouraged by several successful "blind tests" where deposit centres have successfully been predicted from distal propylitic settings. Industry adoption is steadily increasing but is restrained by a lack of the necessary analytical equipment and expertise in commercial laboratories.

INTRODUCTION

The past decade saw a dramatic ramp up in global exploration expenditure in its first half, followed by an equally dramatic decline in expenditure in the latter half, accompanied by one of the harshest downturns in the mining sector in living memory. Over this time, discovery rates have simply not matched the record levels of expenditure (Figure 1), and those discoveries being made were increasingly in areas of post mineral cover and at increasing depth (Schodde, 2017). Never before has it been so important to have effective geochemical exploration tools, but the challenge in developing and applying them is significant. Geochemical exploration is undoubtedly most effective when searching for outcropping or near-surface mineralization in residual terrains. As exploration increasingly focusses on deeper targets and moves inexorably into areas of post-mineral cover, the role of geochemistry in exploration programs is changing.

New geochemical techniques and technologies are urgently needed or the role of geochemistry in making new discoveries will continue to decline. Porphyry-related copper, gold and molybdenum deposits, and their related epithermal gold, silver ± copper ore zones, continue to be attractive exploration targets, with a notable increase in discoveries under cover in the past two decades. Advances in geophysical exploration techniques, combined with deep drilling, have contributed to several spectacular examples of recent porphyry deposit discoveries.

In "Proceedings of Exploration 17: Sixth Decennial International Conference on Mineral Exploration" edited by V. Tschirhart and M.D. Thomas, 2017, p. 457–470

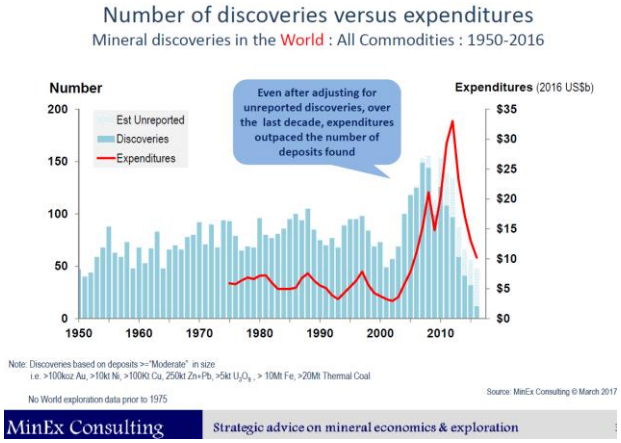

Figure 1: Discovery rate versus exploration expenditure from 1950–2015 (Schodde, 2017).

Geochemical exploration techniques have mostly failed to have the same impact as geophysical exploration methods during this period, due partly to the challenges associated with modification or destruction of hypogene geochemical anomalies by supergene phenomena, and also because of difficulties detecting anomalies beneath syn- and post-mineralization cover. Cost-effective geochemical exploration programs need to maximize the information that can be obtained in early exploration stages. This is particularly true in exploration settings on the edge of cover or when targeting deeper porphyry systems. In these increasingly common scenarios, conventional geochemical signals are weak, alteration is distal, erratic and difficult to separate from background sources with very similar mineral assemblages. Cost effective, low density geochemical techniques that rapidly focus exploration activity into proximal settings are of real value to Industry. The UNCOVER initiative in Australia has identified further development of geochemical tools such as these, a national priority in the AMIRA UNCOVER Roadmap (Rowe, 2017).

Recently, significant efforts have been expended in mineral chemistry research, aimed at aiding porphyry exploration. The recognition of fertile belts of igneous intrusions and prospective areas of hydrothermal alteration can now be assisted through the use of porphyry indicator minerals (PIMS) such as zircon, plagioclase, apatite, magnetite and tourmaline (Dupuis and Beaudoin, 2011; Dilles et al., 2015; Shen et al., 2015; Williamson et al., 2016; Bouzari et al., 2016). At the district scale, far-field detection of concealed mineralized centres in porphyry districts can now be enabled through the application of porphyry vectoring and fertility tools (PVFTS), which involves detection of low-level geochemical anomalies preserved in hydrothermal alteration minerals such as epidote, chlorite or alunite (Chang et al., 2011; Cooke et al., 2014a, 2015, 2017; Wilkinson et al., 2015, 2017; Baker et al., 2017; Xiao et al., 2017). This new generation of geochemical exploration tools has arisen thanks to advances in laser ablation-inductively coupled plasma mass spectrometry (LA-ICP-MS) analytical techniques.

This article reviews new advances in PIMS and PVFTS research in the context of the porphyry exploration model, highlighting how these new tools can add value to exploration campaigns for porphyry deposits. Key aspects of porphyry deposits are also reviewed to provide context for the discussion of PIMS and PVFTS.

PORPHYRY DEPOSITS

Porphyry deposits are the world's largest repositories of copper and molybdenum, and are major sources of gold and silver. Peripheral mineralization styles (e.g., skarns, carbonate replacement deposits and epithermal veins) can be enriched in zinc, lead and silver. Some porphyry deposits are significantly endowed with tin and/or tungsten. Porphyry deposits remain one of the key exploration targets for major mining companies. Their characteristics are well-documented (Sillitoe, 1989, 2000, 2010; Seedorff et al., 2005; Cooke et al., 2014b) and exploration models are well-developed (Lowell and Guilbert, 1970; Gustafson and Hunt, 1975; Holliday and Cooke, 2007). The following sections review key aspects of porphyry deposits and their environments of formation that are pertinent to a discussion of PIMS and PVFTS.

Geodynamic Settings

Most porphyry deposits have a spatial and temporal association with active plate margins (Figure 2). The continental arc settings of South and North America (Figures 2A and C) have been particularly productive for the formation of giant porphyry copper- molybdenum deposits since the Cretaceous. Tertiary and Quaternary oceanic arc settings in the southwst Pacific (Figure 2F), Central America and the Caribbean (Figure 2C) and parts of the Tethyan belt (Figure 2D) have produced significant copper-gold porphyry deposits. Porphyry deposits have also formed in collisional settings such as China and Papua New Guinea (Hou et al., 2009, 2011; Richards, 2009, 2011a; Haschke et al., 2010; Pirajno and Zhou, 2015; Figures 2D and F). Back-arc environments have also been favorable for alkalic porphyry deposits (Hollings et al., 2011; Wolfe and Cooke, 2011).

Porphyry deposits typically form in environments that promote rapid uplift and exhumation (Cooke et al., 2005; Hollings et al., 2005). The deposits therefore have a low preservation potential in the ancient rock record (Wilkinson and Kesler, 2006; Kesler and Wilkinson, 2008; Yanites and Kesler, 2015), with most of the known porphyry deposits being Cretaceous, Tertiary or Quaternary in age. Older examples are known—for example, Paleozoic porphyry deposits are exposed in the Central Asian orogenic belt (Shen et al., 2015; Figure 2E), eastern Australia (Harris et al., 2013; Figure 2G) and Canada (Shelton, 1983), Mesozoic porphyry deposits are well-exposed in western Canada (Bissig and Cooke, 2014; Figure 2C) and Paleoproterozoic examples are preserved in Sweden (Figure 2D). These are generally porphyry deposits that formed in oceanic arc settings that were subsequently amalgamated to continental margins, with a transition of geodynamic settings from those promoting uplift and exhumation to those promoting burial being essential for their preservation.

Several countries and continents apparently lack porphyry deposits, despite being sites of modern or ancient subduction.

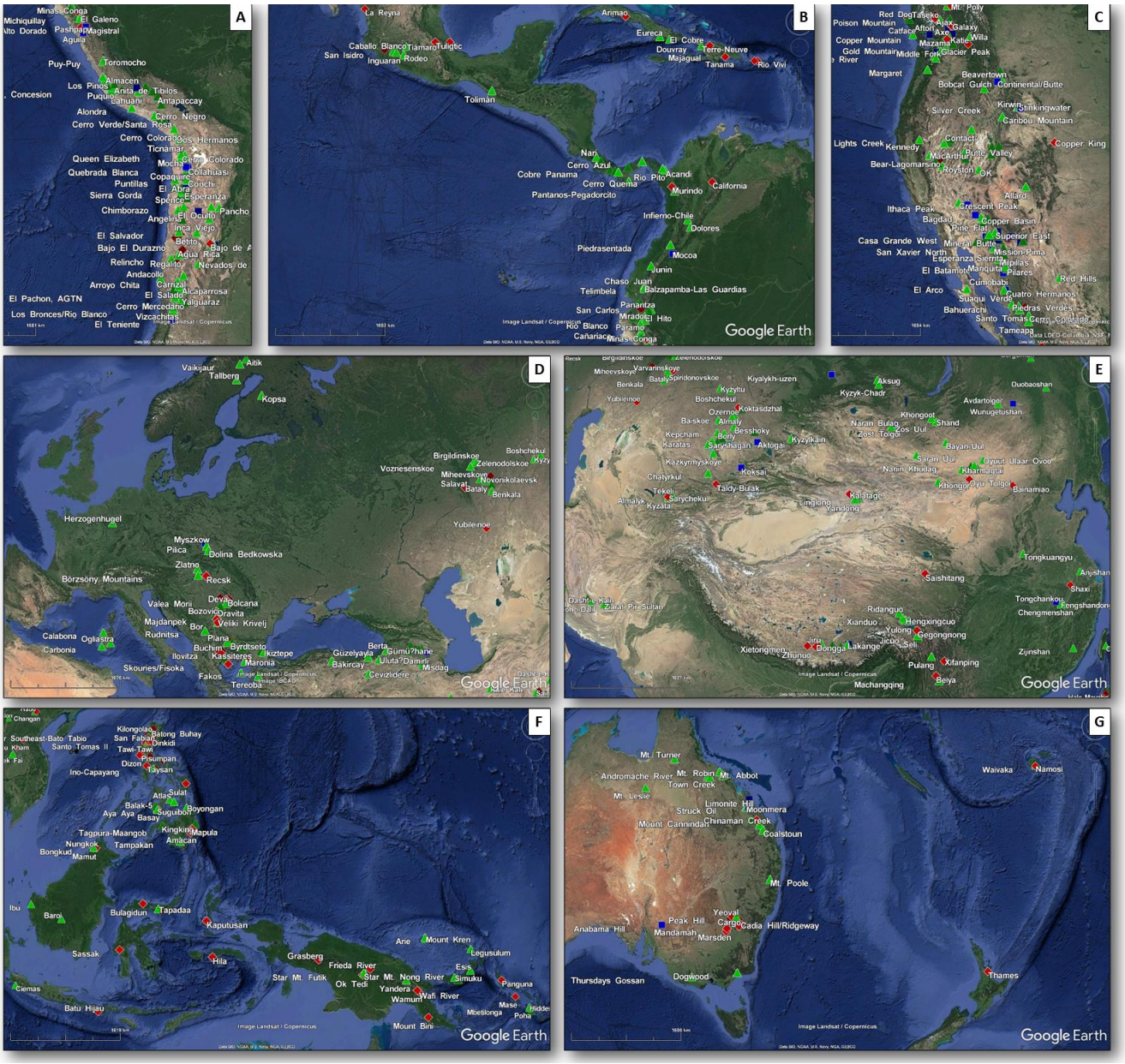

Figure 2: Global distribution of porphyry deposits. (A) South America – most of the porphyry deposits in this region are Cretaceous to Paleocene in age and have formed in an active continental margin setting. This setting has produced most of the world's giant porphyry copper deposits. (B) Central America has porphyry deposits that formed in both continental and island arc settings. (C) North America – most of the largest deposits are Paleocene in age and formed in the southwest USA and northwest Mexico. Mesozoic porphyry deposits of Canada formed in oceanic island arc settings that were accreted to North America, or in post-amalgamation settings. (D) Europe hosts porphyry deposits of the Tethyan belt, a complex collage of continental and island arc environments of Cretaceous to Tertiary ages. There are also Paleoproterozoic deposits exposed in northern Sweden. (E) In Asia, there are Paleozoic deposits of the Central Asian Orogenic Belt, pre-collisional arc-related Mesozoic deposits of the Gandese belt in Tibet, and post-collisional Cretaceous deposits that formed in southwestern China and the Middle-Lower Yangtse river region of eastern China. (F) The southwest Pacific contains numerous porphyry copper-gold deposits that formed in oceanic island arcs in the Philippines, Indonesia and PNG. It has been particularly productive for gold-rich porphyry deposits. There are also examples of continental arc and post-collisional porphyry deposits in New Guinea. (G) Paleozoic oceanic arc-related post-collisional porphyry copper-gold deposits were amalgamated to the Australian craton in southeast Australia. Paleozoic to Mesozoic continental arc settings produced porphyry deposits in northeast Australia. Porphyry deposits are lacking in New Zealand. Deposit names and locations from the USGS porphyry copper database (https://mrdata.usgs.gov/porcu/). Google Earth map data: ©2017 Google, SIO, NOAA, U.S. Navy, NGA, and GEBCO. Green triangles – porphyry copper deposits. Blue squares – porphyry copper-molybdenum deposits. Red diamonds – porphyry copper-gold deposits.

Notable examples in young arc-related settings include New Zealand (Figure 2G) and Japan. The continent of Africa and subcontinent of India are underendowed with porphyry deposits—it remains an open question as to whether this is due to preservation issues, if these terrains were unfavorable for porphyry ore formation, or that they remain comparatively underexplored. Porphyry-style mineralization has been reported from the Antarctic Peninsula (Rowley et al., 1975; Hawkes and Littlefair, 1981), but the United Nations' Antarctic-Environmental Protocol prevents modern exploration of this potentially fertile terrain.

Intrusive Complexes

Porphyry deposits take their name from shallow-crustal porphyritic intrusive complexes that are spatially, temporally and genetically related to porphyry-style alteration and mineralization. A large range of intrusive compositions have produced porphyry mineralization, with individual deposits associated with intermediate (diorite, quartz diorite) to felsic (monzonite, granodiorite, granite) compositions (Kesler et al., 1975; Seedorff et al., 2005; Audetat and Simon, 2012). Tonalites and syenites are also known to be associated with porphyry ores. Generally, copper porphyries are associated with monzonites, granites and syenites, gold porphyries with diorites, molybdenum-porphyries with monzonites, granites and trondhjemites, and tin- Tungsten porphyries with rhyolites and rhyodacites (Seedorff et al., 2005). Although a diverse spectrum of magmatic compositions has produced mineralization, we highlight a few key common characteristics that impact on porphyry exploration.

Porphyry deposits are typically associated with calc-alkaline to alkalic magmas that have intermediate to felsic compositions (Lang et al., 1995; Seedorff et al., 2005). The ultimate source of the shallow level intrusions is thought to be mafic arc magmas formed from low degrees of partial melting and the melting of magmatic sulphides in the lower crust (Hou et al., 2011; Audétat and Simon, 2012). Oxidized magmas are essential for effective magmatic transport of copper, gold and molybdenum together with sulphur from the metasomatised mantle to the upper crust (Richards, 2015). The magmas are sulphur-bearing I-type, magnetite-series intrusions. Sulphur is transported primarily as SO_2 in the melt, preventing sequestration of chalcophile elements into immiscible sulphide droplets and thereby promoting co-transport with copper, gold and molybdenum. The oxidized state of the magmas is reflected in the presence of primary magnetite as phenocrysts and/or groundmass phases. If the intrusive complex exsolved hydrothermal fluids, a domain of magnetite-bearing veins and alteration assemblages may form in and around the intrusive complex, particularly if it has an intermediate composition, with obvious implications for geophysical exploration (Holliday and Cooke, 2007).

The intrusive complexes that produce porphyry deposits generate enormous volumes of magmatic-hydrothermal fluids. This requires extreme water contents in the melts (Richards, 2011b; Loucks, 2014). These hydrous melts can be recognized in the field by the presence of hornblende as a phenocryst phase. Stabilization of hornblende before plagioclase during the magmatic crystallization sequence can potentially produce adakite-like geochemical signatures, which may aid in greenfields exploration (Loucks, 2014; Figure 3). The simple recognition of hornblende as a phenocryst phase in intrusive complexes can be a favorable sign for the prospectivity of a suite of magmatic rocks for porphyry mineralization. Loucks (2014) and Richards (2011b) have suggested whole rock Sr/Y and V/Sc ratios can be used as proxies for high water contents in a magmatic system and consequently their potential to form porphyry systems. For example, Loucks (2012) showed that more than 80 porphyry copper deposits worldwide may be genetically related to felsic intrusions with $Sr/Y > 35$.

Alteration Assemblages

Porphyry-related alteration models are amongst the most utilized and robust in the geoscience discipline, and have facilitated exploration and discovery over half a century. The latter half of this decade has seen the emergence of hyperspectral core scanning technology (Hylogger^{TM}, Corescan^{TM} and TerraCore^{TM}). These technologies, supported by hyperspectral hand-held devices for spot measurements, have delivered a step-change is capacity to robustly recognize and semi-quantify a wide range of spectrally active minerals at a resolutions as low at 500 um. Industry use of these technologies has centred mostly on porphyry and epithermal exploration, although the technology is used across many commodities. Figure 3 highlights key alteration domains associated with mineralized porphyry complexes (Lowell and Guilbert, 1970; Gustafson and Hunt, 1975; Sillitoe, 2000, 2010; Seedorff et al., 2005). These models have proven highly effective for exploration vectoring into proximal setting and this can only be enhanced as the growing volume of high resolution hyperspectral mineralogy expands our understanding of the true complexity of alteration assemblages as well as their vectoring and fertility potential.

Potassic Core

There is typically a central domain of potassic alteration that develops in and around the mineralizing stock. The alteration is characterized by orthoclase, biotite, magnetite, quartz and anhydrite, spatially associated with quartz veins that contain chalcopyrite, bornite, gold and/or molybdenite. This domain is typically the host to high-grade mineralization and is the principal target in porphyry exploration. It may be overprinted by younger clay- and/or muscovite-rich alteration assemblages that can contain significant mineralization, or may dilute or destroy grade.

Green Rock Environment

The potassic core is surrounded laterally by rocks that have undergone propylitic alteration, which can be divided into three subzones (Figure 3). The inner propylitic subzone is rarely recognized, but is defined by the presence of actinolite, together with epidote, chlorite, calcite, albite ± hematite ± pyrite. This passes laterally outwards to the epidote subzone, which lacks actinolite, and then to the outer chlorite subzone, which lacks both actinolite and epidote. These subzones essentially map the actinolite and epidote isograds (Figure 3), and represent decreasing fluid temperatures and oxygen fugacity away from the intrusive complex (Cooke et al., 2014a). Magnetite and

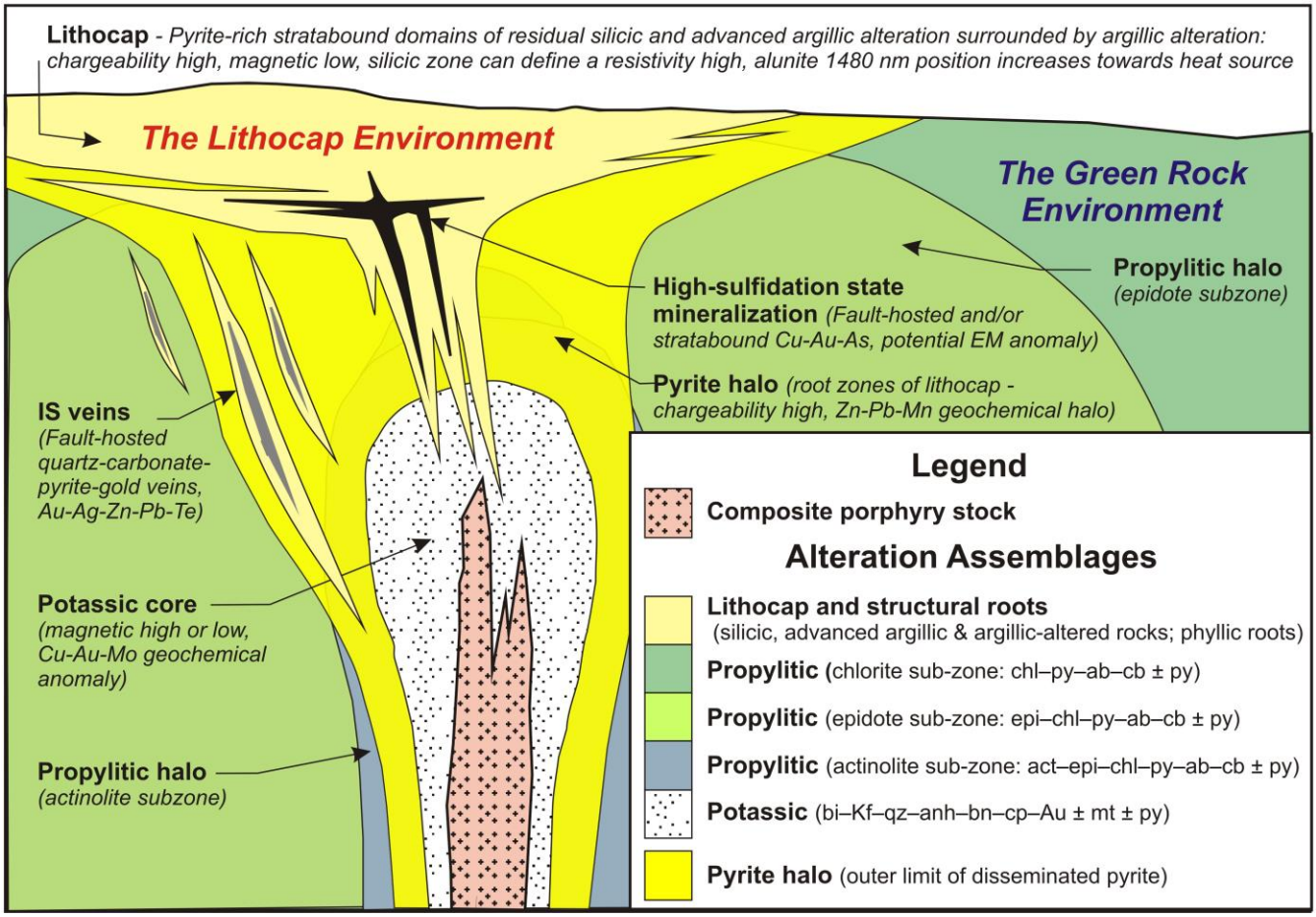

Figure 3: Schematic illustration of alteration zoning and overprinting relationships in a porphyry system (modified after Holliday and Cooke 2007; Cooke et al. 2014b, 2017). The multiphase intrusive complex at the centre of porphyry deposits typically has potassic alteration developed within and around it. The potassic domain may contain magnetite as a vein and/or alteration mineral, particularly when the intrusive complex has mafic to intermediate compositions. The potassic domain passes outwards laterally to three subfacies of propylitic alteration in volcanic rocks: inner high temperature actinolite subzone; intermediate temperature epidote subzone, and outer low temperature chlorite subzone. Sulphides in the porphyry deposit are typically zoned from a central bornite and/or chalcopyrite-rich domain outwards to a pyrite halo. The dimensions of the pyrite halo vary from deposit to deposit, depending on the amount of sulphur released from the intrusive complex and the oxidized or reduced nature of the country rocks. The pyrite halo typically extends into the epidote subzone of the propylitic zone. At shallow levels, a lithocap may overlie and partially overprint porphyry-style mineralization. The lithocap may host high sulphidation-state mineralization and can cover intermediate sulphidation state epithermal veins. The lithocaps will overprint and be surrounded by propylitic alteration assemblages. The roots of the lithocap lie within the pyrite halo of the porphyry system. The degree of superposition of the lithocap into the porphyry system is contingent on uplift and erosion rates at the time of mineralization, and will vary from province to province, and from district to district. Abbreviations: ab – albite; act – actinolite; anh – anhydrite; Au- gold; bi – biotite; bn – bornite; cb – carbonate; chl – chlorite; cp – chalcopyrite; epi – epidote; gt – garnet; hm – hematite; Kf – K-feldspar; mt – magnetite; py – pyrite; qz – quartz.

pyrite may be present as alteration minerals in both the actinolite and epidote subzones, but are best developed close to the intrusive complex, defining magnetite and pyrite alteration halos that can be detected using magnetic and induced polarization (IP) surveys, respectively. Pyrite typically has a broader lateral dispersion than magnetite, so that porphyry deposits can have central magnetic highs surrounded by magnetite lows and variable chargeability anomalies, depending on the sulphide abundances, level of erosion and degree of overprinting by late-stage alteration assemblages. If reactive rocks such as limestones, dolomites, basalts, or ultramafic or silica-undersaturated volcanic rocks are present, then calc-silicate (skarn) alteration assemblages may form around the intrusive complex. Garnet, pyroxene and wollastonite are diagnostic alteration minerals, with retrograde epidote, amphibole, magnetite – hematite, chlorite, calcite, quartz and sulphides common as overprinting phases (Meinert et al., 2005).

Lithocaps

Lithocaps may form between the mineralizing intrusive complex and the paleosurface (Figure 3). Lithocaps are large, stratabound domains of silicic, advanced argillic and argillic alteration assemblages that can exceed dimensions of 10 x 10 km laterally and may be more than 1 km thick (Sillitoe, 1995; Chang et al., 2011; Cooke et al., 2017). Lithocaps typically have structural roots, with advanced argillic assemblages transitioning downwards from quartz – alunite – pyrite to quartz – dickite – pyrophyllite – pyrite and then into phyllic-altered roots (i.e., quartz – muscovite – pyrite; Sillitoe, 1999). Lithocaps provide significant challenges for explorers because they have very broad, difficult to detect lateral alteration zonation patterns defined by clay minerals (Chang et al., 2011). Portable short-wave infrared detectors are essential aids when mapping and exploring lithocaps, as they facilitate the identification of fine grained clays and alunite and help with the detection of alteration zonation patterns.

PORPHYRY INDICATOR MINERALS (PIMS)

The chemical compositions of magmatic and hydrothermal minerals related to porphyry copper deposits can be distinctive relative to the same minerals in the surrounding rocks, and also differ from those related to other mineralization styles, and can be considered as PIMS. Kimberlitic indicator minerals (KIMS) have been intensively used in the diamonds exploration industry since the early 1980s and have been instrumental in the discovery of many of the world's diamond deposits. PIMS have similar potential to assist in the discovery of porphyry copper systems either poorly exposed or eroded and concealed under post-mineral cover. This decade has seen the first use of SEM-based automated mineralogy technology such as MLA^{TM} and QEMSEM^{TM} for exploration purposes. Layton-Matthews et al (2014) demonstrated the value of automated mineralogy on fine fraction till heavy mineral concentrates for detection of glacial indicator mineral trains associated with volcanic-hosted massive sulphide (VHMS)-style deposits. Whilst industry use of automated mineralogy for exploration remains focused on a few early adopters, there is a significant opportunity in the coming decade to greatly enhance the utility and cost effectiveness of PIMS. There are two main categories of PIMS—those that are indicative of potentially fertile magmatic suites, such as zircon, plagioclase and apatite (Shen et al., 2015; Williamson et al., 2016; Bouzari et al., 2016; Loader et al., 2017), and resistate hydrothermal minerals that may be preserved in eroded materials (e.g., stream sediments, soil, till), such as tourmaline, garnet, epidote, pyrite, magnetite, andradite, gold and rutile (Kelley et al., 2011; Eppinger et al., 2013). Some PIMS can be used to discriminate magmatic and hydrothermal environments (e.g., magnetite, apatite, titanite; Dupuis and Beaudoin, 2011; Dare et al., 2014; Celis et al., 2014; Pisiak et al., 2017). We briefly review the characteristics of zircon, plagioclase, apatite and magnetite below.

Zircon

The intermediate to felsic intrusive complexes that produce porphyry copper deposits typically contain zircon as a magmatic accessory phase. Zircon is a key mineral for analysis in porphyry environments, both because it provides the most robust high temperature geochronometer available for magmatic rocks (von Quadt et al. 2012; Chiaradia et al., 2013; Buret et al., 2016, 2017), and also for the profound insights into magma petrogenesis that can be gained from analyses of its isotopic and trace element compositions. Key information gained from trace elements in zircons include: (i) magmatic oxidation states from Ce and Eu anomalies (Ballard et al., 2002; Hoskin and Schaltegger, 2003; Burnham and Berry, 2012; Dilles et al., 2015; Shen et al., 2015), (ii) the temperature of zircon crystallization from Ti content (Ferry and Watson, 2007; Watson and Harrison, 2005), and (iii) evolving magma composition from variations in Zr/Hf, U, Th and Rare Earth Element (REE) patterns (Claiborne et al., 2006; Kemp et al., 2007).

Positive Ce anomalies and negative Eu anomalies in zircon are indicative of oxidized magmas (Ballard et al., 2002; Dilles et al., 2015). In their study of a range of large and small (in terms of copper endowment) Paleozoic porphyry copper-gold deposits of the Central Asian Orogenic Belt, Shen et al. (2015) documented a relationship between the oxidation state of the magmas, as recorded by the Ce^{4+}/Ce^{3+} ratio of zircons, and the copper endowment of the deposit. The intermediate to large deposits all have Ce^{4+}/Ce^{3+} ratios above 120, whereas the small deposits and a comparative dataset of barren Paleozoic granitoids of the Lachlan Fold belt of Australia (Belousova et al., 2006) have much lower Ce^{4+}/Ce^{3+} ratios (Figure 4). It is also important to note that Ce and Eu anomalies in zircon are strongly dependent on melt REE contents, which are usually poorly constrained, and are also controlled by the crystallization of titanite and other REE-bearing phases. Consequently, they are not regarded as especially robust proxies for melt oxidation state (Loader et al., 2017). Nonetheless, on-going research needs to test whether this relationship can be taken to other porphyry provinces globally, or if it is terrane-specific. The combination of zircon trace element chemistry and whole rock geochemistry is likely to be a focus of companies seeking as-yet unrecognized fertile porphyry-bearing belts in underexplored terrains.

Plagioclase

Magmatic plagioclase is abundant as both a phenocryst and groundmass phase in porphyry-related intrusive complexes (Seedorff et al., 2005). Hydrothermal albite is a common alteration product in parts of porphyry systems. Calcic plagioclase occurs more rarely as a hydrothermal phase, particularly in skarns and calc-sodic alteration assemblages (Dilles and Einaudi, 1992). Magmatic plagioclase is commonly altered by hydrothermal processes, and may be replaced by orthoclase (e.g., potassic zone), albite, epidote and/or calcite (e.g., propylitic zone), muscovite/illite (phyllic zone), alunite, pyrophyllite, dickite and/or kaolinite (advanced argillic zone). It is therefore uncommon to find magmatic plagioclase compositions well-preserved in the core of porphyry copper environments. The reactive and commonly altered nature of plagioclase, coupled with its low density, limits its potential as a resistate mineral in exploration.

Magmatic plagioclase has potential to be used as a PIM. Williamson et al. (2016) noted that igneous plagioclase from the world's largest (in terms of contained copper metal) porphyry

copper-molybdenum district, Rio Blanco – Los Bronces (Chile), had excess Al contents when compared to typical arc magmas from the Caribbean that are unrelated to porphyry copper deposits (Figure 5). The excess Al is interpreted to be related to high magmatic water contents that were produced by injection of hydrous fluids or fluid-rich melts into the parental magma chamber (Williamson et al., 2016). Elevated H_2O contents in porphyry ore-forming magmas are an essential prerequisite for porphyry mineralization (Loucks, 2014). Along with whole rock geochemistry and zircon trace element geochemistry, plagioclase compositions may therefore contribute to prospectivity assessments in greenfields targeting exercises. There are, however, two important caveats to this approach: (1) the plagioclase must have pristine magmatic compositions—it cannot be weakly altered or weathered, and (2) the analytical method must be high quality, as the plagioclase compositional variations between fertile and barren intrusions are small and analytical errors could create issues with detection.

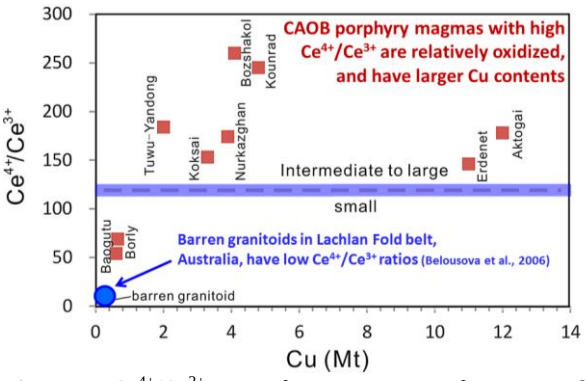

Figure 4: Ce^{4+}/Ce^{3+} ratios for zircon grains from mineralized intrusive complexes versus Cu tonnage (reserves plus past production) of the related porphyry copper deposits from the Central Asian Orogenic Belt (CAOB). The red boxes represent average ratios of zircon from each rock sample. Diagram modified from Shen et al. (2015).

Apatite

Apatite can form in diverse geological environments, including magmatic and hydrothermal settings (Belousova et al., 2002; Hughes and Rakovan, 2015; Webster and Picoli, 2015). Mao et al. (2016) showed that discriminant projection analyses can effectively distinguish apatite from magmatic and a variety of hydrothermal environments, including porphyry, skarn, epithermal, Kiruna, iron oxide copper gold (IOCG) and orogenic deposits. Furthermore, they were able to define distinctive compositions of apatites from various subtypes of porphyry deposits (i.e., Cu Mo Au, Mo and alkalic Cu-Au) and skarn deposits (W vs. Au-Co, Cu and Pb-Zn skarns). It has been shown that both apatite mineral chemistry and apatite luminescence can discriminate magmatic apatite and several varieties of hydrothermal apatite from different alteration zones in selected porphyry deposits of British Columbia (Bouzari et al., 2016; Figure 6) and at Oyu Tolgoi and Resolution (Loader, 2017). These studies highlight that apatite has considerable potential as a PIM.

Magnetite

Magnetite has been considered a prospective indicator mineral for many years due to its resistive nature and ease of separation. Cross (2000) showed that major element ratios (Al//Ti vs V/Ti) could effectively discriminate magmatic and hydrothermal magnetites from porphyry and skarn deposits, and that the hydrothermal environments of magnetite alteration (porphyry vs skarn) could also be discriminated. Dupuis and Beaudoin (2011) took this further, arguing that major element chemistry (e.g., plots of Ca + Al + Mn vs Ti + V) can effectively discriminate magnetite from a diversity of ore deposit types. Using Reko Diq (Pakistan) as an example, Dupuis and Beaudoin (2011) highlighted that individual magnetite compositions may plot in several fields, but the average of these compositions plots in the relevant field for the deposit type of interest. Hu et al. (2015) showed that re-equilibration of magnetite from a single iron skarn deposit in China had produced magnetite compositions that plotted across several of the discrimination fields defined by Dupuis and Beaudoin (2011), highlighting potential challenges with this approach. Distinguishing magmatic and hydrothermal magnetite appears effective, but being able to robustly discriminate different types of hydrothermal magnetite remains a work in progress.

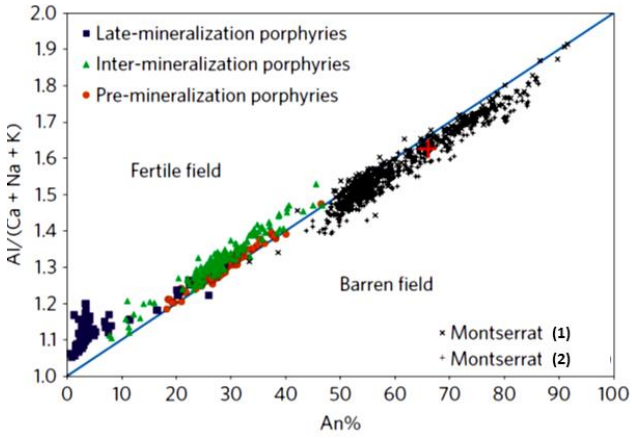

Figure 5: Magmatic plagioclase compositions from pre-, inter- and late-mineralization porphyry intrusions from La Paloma and Los Sulfatos ore zones, Rio Blanco-Los Bronces-Los Sulfatos district Chile. Also shown for comparative purposes are plagioclase compositions from the barren Monserrat volcano, Caribbean. Diagram modified from Williamson et al. (2016). Data sources: 1 - Williamson et al. (2016), 2 – Zelmer et al. (2003).

Dare et al. (2014), Nadoll et al. (2015) and Pisiak et al. (2017) acquired major and trace element analyses of magnetite from a variety of igneous, porphyry and skarn environments. They used element ratios and statistical data exploration to demonstrate how magnetite compositions can effectively discriminate magnetite of diverse origins (e.g., Figure 7). These studies inspire confidence that magnetite has considerable potential as a PIM. There are potentially significant challenges with analyzing magnetite via LA-ICP-MS, because fine exsolution lamellae can affect attempts to analyze it via the LA-ICP-MS technique. If lamellae are ablated together with magnetite, this can impact

adversely on the acquisition of low-level trace element data, and so the analytical approach, and, in particular, quality control during data processing are essential for the acquisition of high-quality uncontaminated data. Another potential issue with magnetite is that it can be prone to diffusional resetting by post-crystallization hydrothermal fluids so that care must be taken in data interpretation. Dare et al. (2012) showed, however, that there are advantages in LA-ICP-MS analyses of magnetite because they provide the average composition of the Fe-oxide precursor prior to exsolution as a consequences of varying P-T-fO_2 conditions, therefore providing the primary signal of the precursor magnetite.

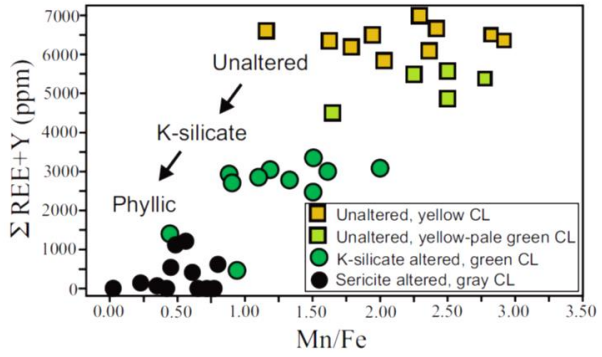

Figure 6: Correlation of apatite luminescence characteristics with the Mn/Fe ratio and abundances of REE in magmatic and hydrothermal apatites from calc-alkaline and alkalic porphyry copper-gold deposits in British Columbia. Reproduced from Bouzari et al. (2016).

PORPHYRY VECTORING AND FERTILITY TOOLS (PVFTS)

Since 2004, a series of AMIRA International research projects (P765, 765A, 1060, 1153) have been conducted at CODES (University of Tasmania) and collaborating organizations. These industry collaborative projects have been robustly supported by up to 21 industry sponsors, several of them over a period of more than 10 years, demonstrating industries sustained interest in this research. The research aims to develop new geochemical and geological methods to detect, vector towards, and discriminate between porphyry and epithermal deposits from different environments. Analysis of subtle, low-level hypogene geochemical signals preserved in hydrothermal alteration minerals can potentially provide explorers with both fertility (how large?) and vectoring information (how far, and in what direction?), allowing the presence, location and significance of porphyry and/or epithermal copper, gold and molybdenum deposits to be assessed during the early stages of exploration with remarkably low-density sampling and very low cost relative to most other available search technologies. These projects have delivered new porphyry vectoring and fertility exploration tools and have demonstrated their efficacy with several successful "blind tests" where deposit centres have successfully be predicted from distal propylitic settings. PVFTS have particular relevance to exploration on the edge of cover, and when drilling under post-mineralization cover, as well as in areas where outcrop is limited (e.g., heavily vegetated tropical settings). Research to date has focused on key alteration minerals in green rock environments (e.g., epidote and chlorite; Cooke et al., 2014a, 2015; Wilkinson et al., 2015, 2017; Baker et al., 2017; Xiao et al., 2017; Figure 3).

Epidote

Epidote is the most visually distinctive mineral in the green rock environment. Its pistachio green color makes it easy to recognize, and it has wide distributions, both as replacement of other Ca-bearing minerals (e.g., plagioclase, hornblende), and as vein fill. Epidote veins can define an outer stockwork around the central quartz-rich stockwork. Mapping of epidote vein intensity can be used to vector towards porphyry centres.

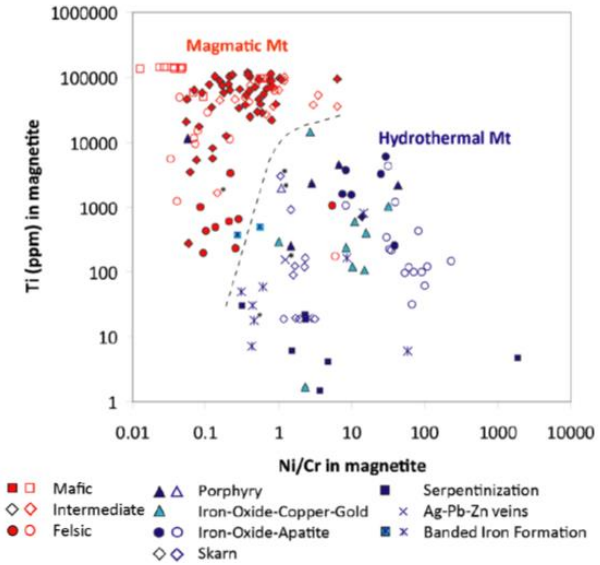

Figure 7: Discrimination of magmatic (red symbols) and hydrothermal magnetite (blue symbols) based on Ti contents and Ni/Cr ratios. Modified from Dare et al. (2014).

In a study of the porphyry copper-gold deposits of the Baguio district, Philippines, Cooke et al. (2014a) showed how the trace element chemistry of epidote can vary with respect to proximity to porphyry mineralized centres, with distal pathfinder elements such as As, Sb and Pb enriched in epidote up to several kilometres away from the porphyry centre. Furthermore, they demonstrated that the pathfinder elements were enriched in epidote around well-endowed (fertile) porphyry centres, and were low in epidote from weakly mineralized prospects. These results imply that epidote LA-ICP-MS analyses have potential both for vectoring and fertility assessments in green rock environments around porphyry deposits. Wilkinson et al. (2017) have shown similar patterns of trace element enrichment and depletion in epidote around the El Teniente porphyry copper-molybdenum deposit, Chile.

LA-ICP-MS analyses can also be used to discriminate between hydrothermal (porphyry-related) and metamorphic epidote. Baker et al. (2017) showed that Sr/As and Pb/U ratios effectively discriminate metamorphic epidotes of Central Chile from porphyry-related epidotes in the same region, and from the Baguio dataset of Cooke et al. (2014a). The metamorphic

epidotes are characterized by very low pathfinder element concentrations (particularly Sb, also As).

Figure 8 shows variations in the As content of epidote from the Taldy Bulak porphyry Cu-Au deposit, Krygystan. Using a broad-spaced sample distribution, LA-ICP-MS analyses of epidote identified a large As low that is coincident with the > 600 ppm Cu in soils anomaly. The advantage of sampling epidote is that it can potentially extend the detectable geochemical footprint of a porphyry deposit by several kilometres. This is likely to be well beyond what is achievable by conventional geochemical sampling techniques such as rock chip, stream sediment and soil geochemistry.

Epidote also has the potential to be used in PIMS exploration (e.g., epidote in till samples; Kelley et al., 2011). It can potentially provide information regarding the presence of proximal or distal porphyry-style propylitic alteration that can then be followed up with PVFTS-style exploration once the bedrock alteration source is identified.

Chlorite

In their study of variations in chlorite compositions around the Batu Hijau porphyry copper-gold deposit, Indonesia, Wilkinson et al. (2015) demonstrated that chlorite effectively provides vectors to the mineralized centre of the deposit within 2.5 km and potentially up to 5 km. Chlorite has proven to be an effective vectoring tool because trace element substitution into the chlorite crystal lattice is strongly controlled by temperature, and probably also by pH, with elements such as Ti, Mg and V enriched in high temperature chlorite, and other elements such as Sr, Li, Co and Ni enriched in chlorite that forms at lower temperatures and/or higher pH. Element ratios (e.g., Ti/Sr; Mg/Sr, V/Ni) enhance the spatial variations and were used to develop 'proximitor' equations (Wilkinson et al., 2017) that can provide vectoring parameters that vary by over four orders of magnitude with distance from the deposit centre. Wilkinson et al. (2017) showed similar results for chlorite analyses from El Teniente, Chile. But in that case, the larger system has produced a larger footprint, with the Ti/Li proximitor able to detect the presence of mineralization up to 5 km from the deposit centre. Wilkinson et al. (2015) commented that the trace element contents of chlorite also show potential as a tool for fertility assessments in porphyry exploration.

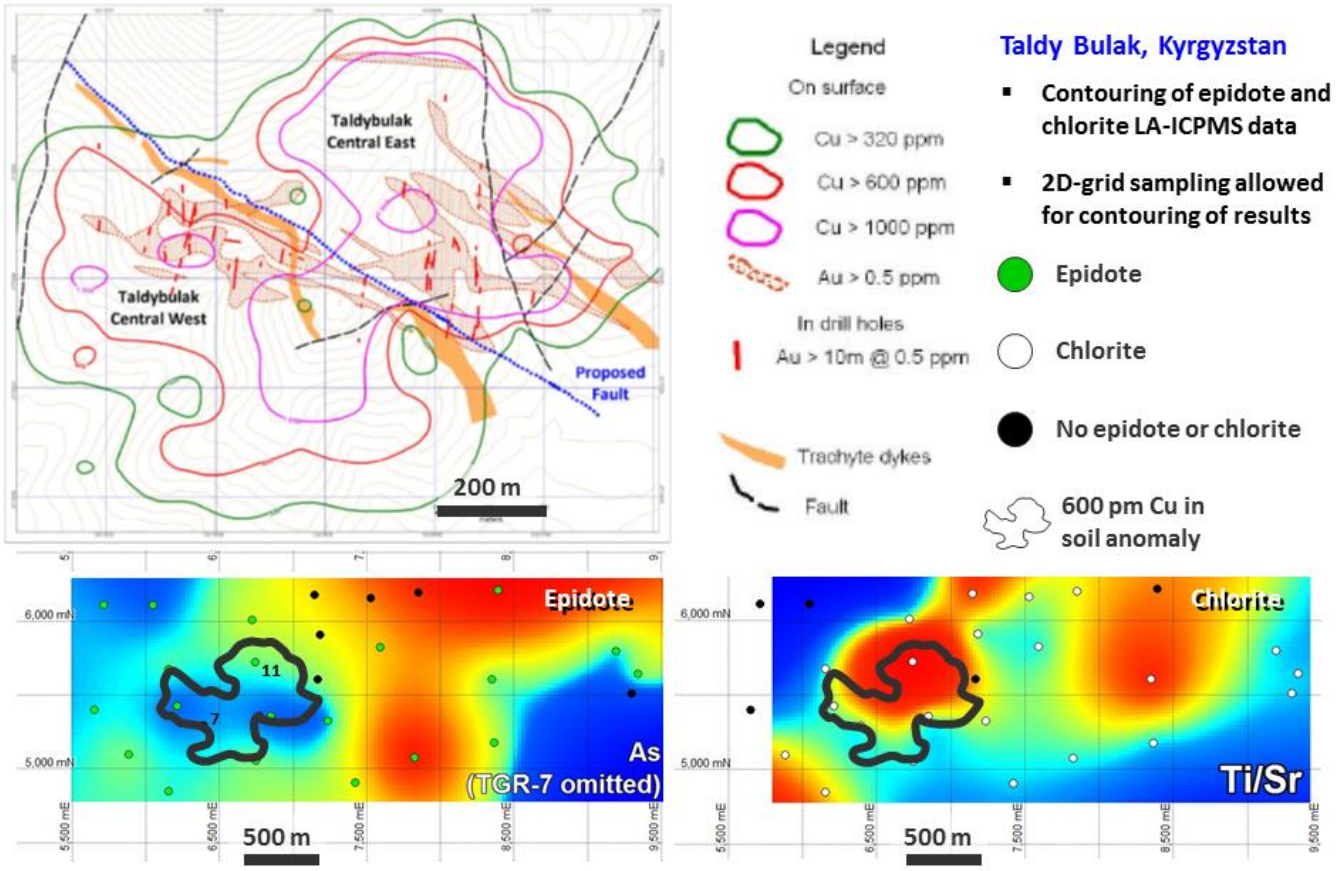

Figure 8: LA-ICP-MS analyses of epidote and chlorite from the Taldy Bulak porphyry copper-gold deposit, Kyrgyzstan, highlights coincident anomalies of low As in epidote and high Ti/Sr ratios in chlorite that coincide with the > 600 ppm Cu in soil anomaly. As in epidote data range from 6.69 to 440 ppm. Ti/Sr ratios for chlorite range from 4.86 to 727. Geological map and Cu assay data from Orsu Metals Corporation – Updated Technical Report on the Taldy Bulak Property, Kyrgyzstan, March 22, 2010.

The combination of epidote and chlorite LA-ICP-MS analyses of samples from green rock environments can help to effectively target porphyry deposits. Figure 8 shows that high Ti/Sr contents of chlorite at Taldy Bulak, Kyrgyzstan, coincide with the As low defined by epidote analyses, and coincide with the 600 ppm Cu in soils anomaly, providing a bulls eye target. A similar response was detected at El Teniente, Chile (Wilkinson et al., 2017). This technology opens up low-cost exploration opportunities on the edge of post-mineral cover or for deep, uneroded porphyry systems including those which may be associated with lithocaps.

Alunite

In the lithocap environment, explorers have been challenged by the huge volumes of intensely altered rocks (silicic, advanced argillic and argillic assemblages; Sillitoe, 1995; Figure 3). In these environments, alteration zonation patterns are difficult to map due in part to the huge scale of the alteration domains, and the challenges associated with accurate field identification of fine grained clay minerals. The advent of portable short wavelength infrared (SWIR) analyzers has transformed exploration in lithocaps, facilitating the mapping of spatial distributions of key alteration minerals such as alunite, pyrophyllite, dickite, illite and kaolinite, which has considerably aided vectoring to porphyry and high sulphidation mineralized centres.

Chang et al. (2011) undertook a systematic study of the Lepanto lithocap, Philippines, which hosts the Lepanto high sulphidation epithermal copper-gold-silver deposit and overlies the Far Southeast copper-gold porphyry deposit. They showed that alunite is a key alteration mineral for exploration in this environment. Alunite has a temperature-dependent solid solution behavior between Na- (high temperature) and K- (low-temperature) end-members (Stoffregen and Cygan, 1990). Chang et al. (2011) showed that the Na and K contents of alunite control the 1480 nm absorption peak position of alunite detected by SWIR techniques. High temperature natroalunite (Na-alunite) has a peak position around 1496 nm, whereas K-alunite has peak positions around 1478. By systematically obtaining SWIR data across the Mankayan lithocap, Chang et al. (2011) demonstrated that higher wavelength values were detected above and near the Far South East porphyry (Figure 9), which is inferred to be the heat and fluid source for the Mankayan lithocap.

Chang et al. (2011) also showed that there are systematic variations in the trace element chemistry of alunite with respect to distance from the Far South East porphyry. Trace elements such as Sr and La are enriched in alunite close to the porphyry, and Pb (which substitutes for K in the alunite crystal structure) is enriched in distal settings. While these mineralogical variations were detected by LA-ICP-MS and microprobe analyses, Chang et al. (2011) showed that the same anomalies could be detected using whole rock geochemistry, provided that rock chip samples were screened using SWIR analysis and whole rock composition, and that only alunite-bearing samples with <0.1% Cu and <0.1 ppm Au were used for plotting spatial variations in vectoring ratios such as 1000000 * Pb/(Na+K), Sr/Pb and 100 * La/Pb (Figure 9).

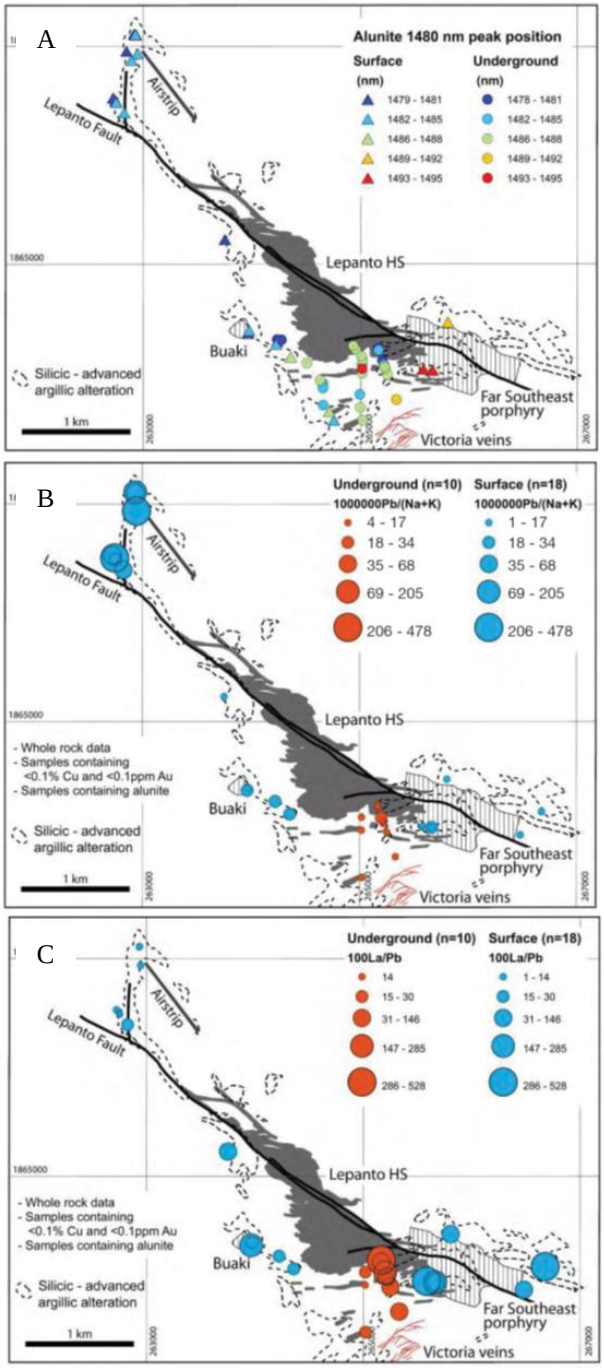

Figure 9: Mankayan lithocap, Philippines. The location of the Lepanto enargite deposit and Far Southeast porphyry copper-gold deposit is shown in grey fill and vertical striped fill, respectively, with surface outcrops of the lithocap marked by dashed lines. (A) Alunite SWIR results. (B) 1000000 * Pb / (Na+K) ratios for whole rock samples. (C) 100 * La/Pb ratios for whole rock samples. All whole rock data screened—only alunite-bearing samples with less than 0.1 % Cu and 0.1 g/t Au plotted. Diagram modified from Chang et al. (2011).

CONCLUSIONS

Several magmatic and hydrothermal minerals show considerable potential as PIMS and/or PVFTS. Several of them are likely to become routine tools used by porphyry explorers over the next decade. However, as commercial labs are yet to embrace LA-ICP-MS technology, and few mining companies have the appropriate in-house analytical facilities, these analyses currently are conducted mostly at university laboratories. Exploration groups including Rio Tinto Exploration and Newcrest Mining have either developed in-house automated mineralogy with LA-ICP-MS capability, or have dedicated access to it. Low-level trace element analyses of PIMS and PVFTS need to be publicly acknowledged to have impacted favorably on a major porphyry discovery in order to validate the approach and to facilitate widespread acceptance of these geochemical exploration techniques. Rio Tinto Exploration has routinely analyzed high volumes of chlorite, epidote and zircon from global porphyry copper exploration programs since 2012 and remains committed demonstrating the importance of this technology (Agnew, 2015).

It has not been an outstanding decade for discovery and industry geoscientists, researches and service providers are going to need to embrace new and emerging technologies if geochemistry is to maintain a critical role in the discovery of new resources.

ACKNOWLEDGEMENTS

We thank all of our research colleagues, sponsors and students (past and present) who have collaborated on AMIRA projects P765, P765A, P1060 and P1153. We thank Andrew Wurst, formerly of Gold Fields, for providing the Taldy Bulak blind site test to AMIRA project P765A. We also thank our AMIRA coordinators, Adele Seymon and Alan Goode, for their tireless support of our work. Georges Beaudoin, John Barr and Charles Beaudry are thanked for their critical comments that have helped to substantially improve this manuscript. The TMVC is an Australian Research Council (ARC)-funded Industrial Transformation Research Hub, and CODES is an ARC Centre of Excellence. The ARC's support of our research is gratefully acknowledged. LODE is generously sponsored by Anglo American, Quantum Pacific Exploration and Rio Tinto. The support of the Natural History Museum and the Department of Earth Science and Engineering at Imperial College London are gratefully acknowledged.

REFERENCES

Agnew, P., 2015, What industry wants from research: Society of Economic Geologists, World Class Ore Deposits – Discovery to Recovery Conference Proceedings, 2 p.

Audétat, A., and A. Simon, 2012, Magmatic controls on porphyry copper genesis: Society of Economic Geologists, Special Publication 16, 553–572.

Baker, M., D.R. Cooke, P. Hollings and J. Piquer, 2017, Identification of hydrothermal alteration related to mineralisation using epidote mineral chemistry: 14th SGA Biennial Meeting, in press.

Ballard, J.R., J.M. Palin, and I.H. Campbell, 2002, Relative oxidation states of magmas inferred from Ce(IV)/Ce(III) in zircon: Application to porphyry copper deposits of northern Chile: Contributions to Mineralogy and Petrology, 144, 347–364.

Belousova, E.A., W.L. Griffin, S.Y. O'Reilly, and N.I. Fisher, N.I., 2002, Apatite as an indicator mineral for mineral exploration: Trace-element compositions and their relationship to host rock type: Journal of Geochemical Exploration, 76, 45–69.

Belousova, E.A., W.L. Griffin, and S.Y. O'Reilly, 2006, Zircon crystal morphology, trace element signatures and Hf isotope composition as a tool for petrogenetic modelling: Examples from Eastern Australian granitoids: Journal of Petrology, 47, 329–353.

Bissig, T. and D.R. Cooke, 2014, Introduction to the special issue devoted to alkalic porphyry Cu-Au and epithermal Au deposits: Economic Geology, 109, 819–825.

Bouzari, F., C. Hart, T. Bissig, and S. Barker, 2016, Hydrothermal alteration revealed by apatite luminescence and chemistry: A potential indicator mineral for exploring covered porphyry copper deposits: Economic Geology, 111, 1397–1410.

Buret, Y., A.V. Quadt, C. Heinrich, D. Selby, M. Wälle, and I. Peytcheva, 2016, From a long-lived upper-crustal magma chamber to rapid porphyry copper emplacement: Reading the geochemistry of zircon crystals at Bajo de la Alumbrera (NW Argentina): Earth and Planetary Science Letters, 450, 120 – 131.

Buret, Y., J.F. Wotzlaw, S. Roozen, M. Guillong, A.V. Quadt, and C. Heinrich, 2017, Zircon petrochronological evidence for a plutonic-volcanic connection in porphyry copper deposits: Geology, 45, 623-626.

Burnham, A.D. and A.J. Berry, 2012, An experimental study of trace element partitioning between zircon and melt as a function of oxygen fugacity: Geochimica et Cosmochimica Acta, 95, 196–212.

Celis, M.A., F. Bouzari, T. Bissig, C.J.R. Hart, and T. Ferbey, 2014, Petrographic characteristics of porphyry indicator minerals from alkalic porphyry copper-gold deposits in south-central British Columbia (NTS 092, 093): Geoscience BC, Summary of Activities 2013, 2014-1, 53–62.

Chang Z, J.W. Hedenquist, N.C. White, D.R. Cooke, M. Roach, C.L. Deyell, J. Garcia, J.B. Gemmell, S. McKnight, and A.L. Cuison, 2011, Exploration tools for linked porphyry and epithermal deposits: Example from the Mankayan intrusion-centered Cu-Au district, Luzon, Philippines: Economic Geology, 106, 1365–1398.

Chiaradia, M., U. Schaltegger, R. Spikings, J.F. Wotzlaw, and M. Ovtcharova, 2013, How accurately can we date the duration of magmatic-hydrothermal events in porphyry systems?—An invited paper: Economic Geology, 108, 565-584.

Claiborne, L.L., C.F. Miller, B.A. Walker, J.L. Wooden, F.K. Mazdab, and F. Bea, 2006, Tracking magmatic processes through Zr/Hf ratios in rocks and Hf and Ti zoning in zircons: An

example from the Spirit Mountain batholith, Nevada: Mineralogical Magazine, 70, 517-543.

Cooke, D.R., P. Hollings, and J. Walshe, 2005, Giant porphyry deposits – Characteristics, distribution and tectonic controls: Economic Geology, 100, 801–818.

Cooke D.R., M. Baker, P. Hollings, G. Sweet, Z. Chang, L. Danyushevsky, S. Gilbert, T. Zhou, N.C. White, J.B. Gemmell, and S. Inglis, 2014a, New advances in detecting systems – epidote mineral chemistry as a tool for vectoring and fertility assessments: Society of Economic Geologists, Special Publication 18, 127–152.

Cooke D.R., P. Hollings, J.J. Wilkinson, and R.M. Tosdal, 2014b, Geochemistry of porphyry deposits, in H.D. Holland and K.K. Turekian, eds., Treatise on Geochemistry, Second Edition, Oxford, Elsevier, 13, 357–381.

Cooke, D.R., J.J. Wilkinson, M. Baker, P. Agnew, C.C. Wilkinson, H. Martin, Z. Chang, H. Chen, J.B. Gemmell, S. Inglis, L. Danyushevsky, S. Gilbert, and P. Hollings, 2015, Using mineral chemistry to detect the location of concealed porphyry deposits – an example from Resolution, Arizona: 27th International Association of Geochemistry Symposium, Conference Proceedings.

Cooke D.R., N.C. White, L. Zhang, Z. Chang, and H. Chen, 2017, Lithocaps – characteristics, origins and significance for porphyry and epithermal exploration: 14th SGA Biennial Meeting, in press.

Cross, A.J., 2000, An investigation of the minor and trace element chemistry of hydrothermal porphyry and skarn-related magnetite: PhD thesis, University of Canberra.

Dare, S.A., S.J. Barnes, G. Beaudoin, J. Méric, E. Boutroy, and C. Potvin-Doucet, 2014, Trace elements in magnetite as petrogenetic indicators: Mineralium Deposita, 49, 785–796.

Dilles J.H. and M.T., Einaudi, 1992, Wall-rock alteration and hydrothermal flow paths about the Ann-Mason porphyry copper deposit, Nevada—a 6-km vertical reconstruction: Economic Geology, 87, 1963−2001.

Dilles, J.H., A.J.R. Kent, J.L. Wooden, R.M. Tosdal, A. Koleszar, R.G. Lee, and L.P. Farmer, 2015, Zircon compositional evidence for sulfur-degassing from ore-forming arc magmas: Economic Geology, 110, 241–251.

Dupuis, C. and G. Beaudoin, 2011, Discriminant diagrams for iron oxide trace element fingerprinting of mineral deposit types: Mineralium Deposita, 46, 319–335.

Ferry, J.M. and E.B. Watson, 2007, New thermodynamic models and revised calibrations for the Ti-in-zircon and Zr-in-rutile thermometers: Contributions to Mineralogy and Petrology, 154, 429–437.

Gustafson, L.B. and J.P. Hunt, 1975, The porphyry copper deposit at El Salvador, Chile: Economic Geology, 70, 857–912.

Harris, A.C., D.R. Cooke, J.L. Blackwell, N. Fox, and E.A. Orovan, 2013, Volcano-tectonic setting of world class alkalic porphyry and epithermal Au ± Cu deposits of the southwest Pacific: Society of Economic Geologists Special Publication 17, 337–360.

Haschke, M., J. Ahmadian, M. Murata, and I. McDonald, 2010, Copper mineralization prevented by arc-root delamination during Alpine-Himalayan collision in Central Iran: Economic Geology, 105, 855–865.

Hawkes, D.D. and M.J. Littlefair, 1981, An occurrence of molybdenum, copper, and iron mineralization in the Argentine Islands, West Antarctica: Economic Geology, 76, 898–904.

Holliday, J.R. and D.R. Cooke, 2007, Advances in geological models and exploration methods for copper ± gold porphyry deposits, in B. Milkereit, ed., Proceedings of Exploration 07, 791–809.

Hollings, P., D.R. Cooke, and A. Clark, 2005, Regional geochemistry of Tertiary volcanic rocks in Central Chile: Implications for tectonic setting and ore deposit genesis: Economic Geology, 100, 887–904.

Hollings, P., R. Wolfe, D.R. Cooke, and P. Waters, 2011, Geochemistry of Tertiary igneous rocks of Northern Luzon, Philippines: Evidence for a back-arc setting for alkalic porphyry copper–gold deposits and a case for slab roll-back?: Economic Geology, 106, 1257–1277.

Hoskin, P.W.O. and U. Schaltegger, 2003, The composition of zircon and igneous and metamorphic petrogenesis: Reviews in Mineralogy and Geochemistry, 53, 27−62.

Hou, Z., Z. Yang, X. Qu, X. Meng, Z. Li, G. Beaudoin, Z. Rui, Y. Gao, and K. Zaw, 2009, The Miocene Gangdese porphyry copper belt generated during post-collisional extension in the Tibetan Orogen: Ore Geology Reviews, 36, 25–51.

Hou, Z.Q., H.R. Zhang, X.F. Pan, and Z.M. Yang, 2011, Porphyry Cu (−Mo–Au) deposits related to melting of thickened mafic lower crust: Examples from the eastern Tethyan metallogenic domain: Ore Geology Reviews, 39, 21-45.

Hu, H., D. Lentz, J.-W. Li, T. McCarron, X.-F. Zhao, and D. Hall, 2015, Re-equilibration processes in magnetite from iron skarn deposits: Economic Geology, 110, 1–8.

Hughes, J.M. and J.F. Rakovan 2015, Structurally robust, chemically diverse: apatite and apatite supergroup minerals: Elements, 11, 165-170

Kelley, K.D., R.G. Eppinger, J. Lang, S.M. Smith, and D.L. Fey, 2011, Porphyry Cu indicator minerals in till as an exploration tool: Example from the giant Pebble porphyry Cu-Au-Mo deposit, Alaska, USA: Geochemistry: Exploration, Environment, Analysis, 11, 321–334.

Kemp, A.I., C.J. Hawkesworth, G.L. Foster, B.A. Paterson, J.D. Woodhead, J.M. Hergt, C.M. Gray, and M.J. Whitehouse, 2007, Magmatic and crustal differentiation history of granitic rocks from Hf-O isotopes in zircon: Science, 315 (5814), 980-983.

Kesler, S.E. and B.H. Wilkinson, 2008, Earth's copper resources estimated from tectonic diffusion of porphyry copper deposits: Geology, 36, 255-258.

Kesler, S., L. Jones, and R. Walker, 1975, Intrusive rocks associated with porphyry copper mineralization in island arc magmas: Economic Geology, 70, 515-526.

Lang, J.R., B. Lueck, J.K. Mortensen, J.K. Russell, C.R. Stanley, and J.F.H. Thompson, 1995, Triassic-Jurassic silica-undersaturated and silica-saturated alkalic intrusions in the Cordillera of British Columbia – implications for arc magmatism: Geology, 23, 451–454.

Layton-Matthews, D., C. Hamilton, and M.B. McClenaghan, 2014, Mineral chemistry: modern techniques and applications to exploration: Application of indicator mineral methods to mineral exploration, 26th International Applied Geochemistry Symposium, Short Course SC07, 9-18.

Loader, M.A., 2017, Mineral indicators of porphyry Cu fertility: PhD thesis, Imperial College London.

Loader, M.A., J.J. Wilkinson, and R.N. Armstrong, 2017, The effect of titanite crystallisation on Eu and Ce anomalies in zircon and its implications for the assessment of porphyry Cu deposit fertility: Earth and Planetary Science Letters, 472, 107-119.

Loucks, R., 2012, Chemical characteristics, geodynamic setting and petrogenesis of copper-ore-forming arc magmas: Centre for Exploration Targeting Quarterly Newsletter, 19, 1–10.

Loucks, R.R., 2014, Distinctive composition of copper-ore-forming arc magmas: Australian Journal of Earth Sciences, 61, 5-16.

Lowell, J.P. and J.M. Guilbert, 1970, Lateral and vertical alteration-mineralization zoning in porphyry ore deposits: Economic Geology, 65, 373-408.

Mao, M., A.S. Rukhlov, S.M. Rowins, J. Spence, and L.A. Coogan, 2016, Apatite trace element compositions: A robust new tool for mineral exploration: Economic Geology, 111, 1187–1222.

Meinert, L.A., G.M. Dipple, and S. Nicolescu, 2005, World skarn deposits: Economic Geology 100th Anniversary Volume, 299–336.

Nadoll, P., J.L. Mauk, R.A. Leveille, and A.E. Koenig, 2015, Geochemistry of magnetite from porphyry Cu and skarn deposits in the southwestern United States: Mineralium Deposita, 50, 493–515.

Pirajno, F. and T. Zhou, 2015, Intracontinental porphyry and porphyry-skarn mineral systems in Eastern China: Scrutiny of a special case “Made-in-China”: Economic Geology, 110, 603-629.

Pisiak, L.K., D. Canil, T. Lacourse, A. Plouffe, and T. Ferbey, 2017, Magnetite as an indicator mineral in the exploration of porphyry deposits: A case study in till near the Mount Polley Cu-Au deposit, British Columbia, Canada: Economic Geology, 112: 919–940.

Richards, J.P., 2009, Postsubduction porphyry Cu-Au and epithermal Au deposits: Products of remelting of subduction-modified lithosphere: Geology, 37, 247–250.

Richards, J.P., 2011a, Magmatic to hydrothermal metal fluxes in convergent and collided margins: Ore Geology Reviews, 40, 1−26.

Richards, J.P., 2011b, High Sr/Y arc magmas and porphyry Cu ± Mo ± Au deposits: Just add water: Economic Geology, 106, 1075–1081.

Richards, J.P., 2015, The oxidation state, and sulfur and Cu contents of arc magmas: implications for metallogeny: Lithos, 233, 27−45.

Rowe, R., 2017, Why and how Uncover?: Presented at Science in the Surveys Conference, 21 p.

Rowley, P.D., P.L. Williams, D.L. Schmidt, R.L. Reynolds, A.B. Ford, A.H. Clark, E. Farrar, and S.L. McBride, 1975, Copper mineralization along the Lassiter Coast of the Antarctic Peninsula: Economic Geology, 70, 982–987.

Schodde, R., 2017, Recent trends and outlook for global exploration: Presented at PDAC.

Seedorff, E., J.H. Dilles, J.M. Proffett Jr., M.T. Einaudi, L. Zurcher, W.J.A. Stavast, D.A. Johnson, and M.D. Barton, 2005, Porphyry deposits: Characteristics and origin of hypogene features: Economic Geology 100th Anniversary Volume, 251–298.

Shen, P., K. Hattori, H. Pan, S. Jackson, and E. Seitmuratova, 2015, Oxidation condition and metal fertility of granitic magmas: Zircon trace-element data from porphyry Cu deposits in the Central Asian orogenic belt: Economic Geology, 110, 1861–1878.

Sillitoe, R.H., 1989, Gold deposits in western Pacific island arcs; the magmatic connection: Economic Geology, Monograph 6, 274–291.

Sillitoe, R.H., 1995, Exploration of porphyry copper lithocaps: AUSIMM Publication Series 9, 527−532.

Sillitoe, R.H., 2000, Styles of high-sulphidation gold, silver, and copper mineralization in porphyry and epithermal environments: The AusIMM Proceedings, 305, 19–34.

Sillitoe, R.H., 2010, Porphyry-copper systems: Economic Geology, 105, 3-41.

Stoffregen, R.E. and G.L. Cygan, 1990, An experimental study of Na-K exchange between alunite and aqueous sulfate solutions: American Mineralogist, 75, 209−220.

Von Quadt, A., M. Erni, K. Martinek, M. Moll, I. Peytcheva, and C.A. Heinrich, 2011, Zircon crystallization and the lifetimes of ore-forming magmatic-hydrothermal systems: Geology, 39, 731−734.

Watson, E.B. and T.M. Harrison, 2005, Zircon thermometer reveals minimum melting conditions on earliest earth: Science, 308, 841−844.

Webster, J.D. and P.M. Piccoli 2015, Magmatic apatite: a powerful, yet deceptive, mineral: Elements, 11, 177-182.

Wilkinson, B.H. and S.E. Kesler, 2006, Tectonism and exhumation in convergent margin orogens: Insights from ore deposits: Journal of Geology, 115, 611–627.

Wilkinson, J.J., Z. Chang, D.R. Cooke, M. Baker, C.C. Wilkinson, S. Inglis, H. Chen, and J.B. Gemmell, 2015, The chlorite proximitor: A new tool for detecting porphyry ore deposits: Journal of Geochemical Exploration, 152, 10–26.

Wilkinson, J.J., M. Baker, D.R. Cooke, C.C. Wilkinson, and S. Inglis, 2017, Exploration targeting in porphyry Cu systems using propylitic mineral chemistry: a case study of the El Teniente deposit, Chile: 14th SGA Biennial Meeting, in press.

Williamson, B.J., R.J. Herrington, and A. Morris, 2016, Porphyry copper enrichment linked to excess aluminium in plagioclase: Nature Geosciences, 9, 237–242.

Wolfe, R. and D.R. Cooke, 2011, Geology of the Didipio region and genesis of the Dinkidi alkalic porphyry Cu–Au deposit and related pegmatites, northern Luzon, Philippines: Economic Geology, 106, 1279–1315.

Xiao, B., H. Chen, Y. Wang, J. Han, C. Xu, and J. Yang, 2017, Chlorite and epidote chemistry of the Yandong Cu deposit, NW China: Metallogenic and exploration implications for Paleozoic porphyry Cu systems in the Eastern Tianshan: Ore Geology Reviews, http://dx.doi.org/10.1016/j.oregeorev.2017.03.004

Yanites, B.J. and S.E. Kesler, 2015, A climate signal in exhumation patterns revealed by porphyry copper deposits: Nature Geoscience, 8, 462–465.

Zellmer, G.F., R.S.J. Sparks, C.J. Hawkesworth, and M. Wiedenbeck, 2003, Magma emplacement and remobilization timescales beneath Montserrat: insights from Sr and Ba zonation in plagioclase phenocrysts: Journal of Petrology, 44, 1413–1431.